

## NANO EXPRESS

## Open Access

# Study of the oxygen vacancy influence on magnetic properties of Fe- and Co-doped SnO<sub>2</sub> diluted alloys

Pablo D Borges<sup>1</sup>, Luisa M R Scolfaro<sup>2\*</sup>, Horacio W Leite Alves<sup>3</sup>, Eronides F da Silva Jr.<sup>4</sup> and Lucy V C Assali<sup>5</sup>**Abstract**

Transition-metal (TM)-doped diluted magnetic oxides (DMOs) have attracted attention from both experimental and theoretical points of view due to their potential use in spintronics towards new nanostructured devices and new technologies. In the present work, we study the magnetic properties of Sn<sub>0.96</sub>TM<sub>0.04</sub>O<sub>2</sub> and Sn<sub>0.96</sub>TM<sub>0.04</sub>O<sub>1.98</sub>(V<sub>O</sub>)<sub>0.02</sub>, where TM = Fe and Co, focusing in particular in the role played by the presence of O vacancies nearby the TM. The calculated total energy as a function of the total magnetic moment per cell shows a magnetic metastability, corresponding to a ground state, respectively, with 2 and 1 μ<sub>B</sub>/cell, for Fe and Co. Two metastable states, with 0 and 4 μ<sub>B</sub>/cell were found for Fe, and a single value, 3 μ<sub>B</sub>/cell, for Co. The spin-crossover energies ( $E_S$ ) were calculated. The values are  $E_S^{0/2} = 107$  meV and  $E_S^{4/2} = 25$  meV for Fe. For Co,  $E_S^{3/1} = 36$  meV. By creating O vacancies close to the TM site, we show that the metastability and  $E_S$  change. For iron, a new state appears, and the state with zero magnetic moment disappears. The ground state is 4 μ<sub>B</sub>/cell instead of 2 μ<sub>B</sub>/cell, and the energy  $E_S^{2/4}$  is 30 meV. For cobalt, the ground state is then found with 3 μ<sub>B</sub>/cell and the metastable state with 1 μ<sub>B</sub>/cell. The spin-crossover energy  $E_S^{1/3}$  is 21 meV. Our results suggest that these materials may be used in devices for spintronic applications that require different magnetization states.

**Keywords:** Tin dioxide, Diluted magnetic semiconductors, Magnetic properties, *ab initio* calculations, Electronic structure

**Background**

Nowadays, dilute magnetic oxides (DMOs) are potential candidates for both spintronic devices and nanodevices applications. Although the existence of room temperature ferromagnetism (FM) in transition metal (TM)-doped SnO<sub>2</sub> has been reported, the origin of the FM is still controversial. There are indications that the FM comes from different sources, metallic clusters, secondary phases, or is due to a free carrier-mediated mechanism in the bulk. The presence of oxygen vacancies is systematically related to the observed ferromagnetic state. These systems are good candidates to obtain materials with a half-metallic behavior, with 100% spin-polarized carriers at the Fermi level.

Tin dioxide (SnO<sub>2</sub>) doped with transition metals (TMs) have been extensively investigated recently due to the resulting important magnetic properties [1-6]. The

ferromagnetic behavior has been observed at room temperature in Cr-, Mn-, Fe- and Co-doped SnO<sub>2</sub> DMO systems [7-12], indicating the potential of such systems for spintronic applications. It has also been observed that the presence of oxygen vacancies appears to be required for producing FM in DMOs, such as, e.g., in Co-doped ZnO [13], in Co-doped TiO<sub>2</sub> [14,15], in Fe- and Co-doping in In<sub>2</sub>O<sub>3</sub> [16,17], and in Fe-, Co-, and Cr- doped SnO<sub>2</sub> [7,18,19]. A theoretical model proposed by Coey et al. to interpret the FM in these semiconducting oxides requires the existence of oxygen vacancies in close proximity to TM sites in order to maintain the charge neutrality [20]. For Cr-doped SnO<sub>2</sub> nanoparticles, the obtained FM behavior is limited by a maximum doping concentration  $x_L$  which has a strong relation with structural changes revealed from X-ray diffraction measurements [7]. The presence of oxygen vacancies in these Sn<sub>1-x</sub>TM<sub>x</sub>O<sub>2</sub> samples, in which the TM concentrations  $x$  varies from 0% to 10%, has been detected by electron paramagnetic resonance experiments [19].

\* Correspondence: [lscolfaro@txstate.edu](mailto:lscolfaro@txstate.edu)<sup>2</sup>Department of Physics, Texas State University, San Marcos, TX 78666, USA  
Full list of author information is available at the end of the article

Many efforts have been made in attempt to characterize and understand the mechanisms involved in the ferromagnetic behavior observed in such systems.

In this work, we study the oxygen vacancy influence on magnetic properties of the Fe- and Co-doped SnO<sub>2</sub> diluted alloys. First, the systems Sn<sub>1-x</sub>MT<sub>x</sub>O<sub>2</sub>, for  $x = 0.04$ , were studied through *ab initio* electronic structure calculations performed within the spin density functional theory. The concentration of  $x = 0.04$  corresponds to a typical experimental value. Second, an oxygen vacancy nearest neighbor to the TM atom in the alloys was introduced. Sn<sub>1-x</sub>TM<sub>x</sub>O<sub>2-y</sub>(V<sub>O</sub>)<sub>y</sub> systems, with  $x = 0.04$  and  $y = 0.02$ , and its consequences for the magnetic behavior of these systems were considered. Finally, an investigation about the magnetic metastability was done, and the spin-crossover phenomenon was studied. A metamagnetic state is the key underlying conceptual mechanism for storage, memory, and display device and nanodevice applications [21], and this work shows that DMO materials based on Fe- and Co-doped SnO<sub>2</sub> taking into account the oxygen vacancy influence could be engineered to display different stable magnetized states.

## Methods

The calculations were based on the spin density functional theory. We employed the projector augmented wave method implemented in the Vienna *ab-initio* simulation package (VASP-PAW) [22,23]. The exchange-correlation potential used was the generalized gradient approximation in the Perdew, Burke, and Ernzerhof [24] approach. The method has been previously used to study the structural and electronic properties of bulk rutile SnO<sub>2</sub> [25]. The valence electronic distributions for the PAWs representing the atoms were Sn  $4d^{10}5s^25p^2$ , Fe  $3d^74s^1$ , Co  $3d^74s^2$ , and O  $2s^22p^6$ . The onsite correction Hubbard  $U$  for Co- and Fe  $d$  orbitals was not considered. Previous calculations for Cr doping SnO<sub>2</sub> taking into account a  $U$  correction show no major changes in our conclusions. Scalar relativistic effects were taken into account. To describe the alloys, we used a 72-atom supercell (24 Sn and 48 O atoms) and a  $4 \times 4 \times 4$  mesh of Monkhorst-Pack  $k$ -points for integration in the Brillouin zone. All the calculations were done with a 490-eV energy cutoff in the plane-wave expansions, and the systems were fully relaxed until the residual forces on the ions were less than 10 meV/Å.

## Results and discussion

We studied the systems Sn<sub>0.96</sub>TM<sub>0.04</sub>O<sub>2</sub> and the Sn<sub>0.96</sub>TM<sub>0.04</sub>O<sub>1.98</sub>(V<sub>O</sub>)<sub>0.02</sub> (with TM = Fe and Co) with the oxygen vacancy as the TM nearest neighbor. In both cases, a single tin atom was substituted with a TM atom

in the 72-atom supercell, simulating the  $x = 0.04$  impurity and  $y = 0.02$  oxygen vacancy concentrations. For all cases, the total energy was calculated for several magnetic moment values.

It was recently shown by us [26] that when a Sn atom is replaced by a chromium atom in SnO<sub>2</sub>, a high-spin (HS) ground state with a magnetic moment  $m = 2 \mu_B$ /cell and a low-spin state (LS) with a magnetic moment  $m = 0 \mu_B$ /cell are obtained. For this case, a spin crossover becomes possible with an energy barrier of 114 meV calculated for the transition from  $m = 0$  to  $2 \mu_B$ /cell. When an oxygen vacancy (out of the six first neighbors of Cr) is considered, the behavior of the total energy versus the magnetic moment per cell showed the appearance of a second HS configuration, with magnetic moment  $m = 4 \mu_B$ /cell and an energy barrier of 32 meV relative to the  $2 \mu_B$ /cell state. The ground state, however, remains as the  $2 \mu_B$ /cell magnetic moment HS state. The energy barrier for the  $m = 0$  to  $2 \mu_B$ /cell transition was reduced to 27 meV. Comparing this value with the one for this barrier in the DMO without the vacancy (114 meV), a drastic transition for the DMO without the vacancy of 114 meV, a drastic reduction by about 75% is observed.

We show here that if a single Sn atom is substituted by a Fe or a Co impurity, the magnetic metastability observed for Cr-doped SnO<sub>2</sub> diluted alloys also occurs. Figure 1a,b shows the total energy behavior for the Sn<sub>0.96</sub>Fe<sub>0.04</sub>O<sub>2</sub> and Sn<sub>0.96</sub>Fe<sub>0.04</sub>O<sub>1.98</sub>(V<sub>O</sub>)<sub>0.02</sub> diluted magnetic alloys, respectively, in function of magnetic moment/cell. A ground state with a magnetic moment  $m = 2 \mu_B$ /cell and two metastable states with magnetic moments of  $m = 0$  and  $m = 4 \mu_B$ /cell were observed for the system without the oxygen vacancy. The crossover energy barrier for the transition from  $m = 0$  to  $2 \mu_B$ /cell is  $E_S^{0/2} = 107$  meV, and for the transition from  $m = 4$  to  $2 \mu_B$ /cell is  $E_S^{4/2} = 25$  meV. When the oxygen vacancy is considered,  $m = 0 \mu_B$ /cell is no longer a metastable state; however, new states appear with magnetic moment varying in the range  $2 \leq m \leq 6$ . The ground state occurs at  $m = 4 \mu_B$ /cell, and two almost flat regions between  $2 \leq m \leq 3.5 \mu_B$ /cell (region R1) and  $4 \leq m \leq 6 \mu_B$ /cell (region R2) are seen. Energy barriers of  $E_S^{2/4} = 30$  meV for the transition from  $m = 2$  to  $4 \mu_B$ /cell and  $E_S^{6/4} = 16$  meV for the transition from  $m = 4$  to  $6 \mu_B$ /cell were observed. Figure 1c,d shows the total energy versus magnetic moment for Sn<sub>0.96</sub>Co<sub>0.04</sub>O<sub>2</sub> and Sn<sub>0.96</sub>Co<sub>0.04</sub>O<sub>1.98</sub>(V<sub>O</sub>)<sub>0.02</sub> alloys, respectively. The ground state for the system without the oxygen vacancy is at  $m = 1 \mu_B$ /cell, and a magnetic metastable at  $m = 3 \mu_B$ /cell is seen. The energy barrier of  $E_S^{3/1} = 36$  meV for the transition from  $m = 3$  to  $1 \mu_B$ /cell was obtained. For the Co-doped SnO<sub>2</sub> with an oxygen vacancy, we obtain a change in the magnetic metastable states: the ground state is at  $m = 3 \mu_B$ /cell

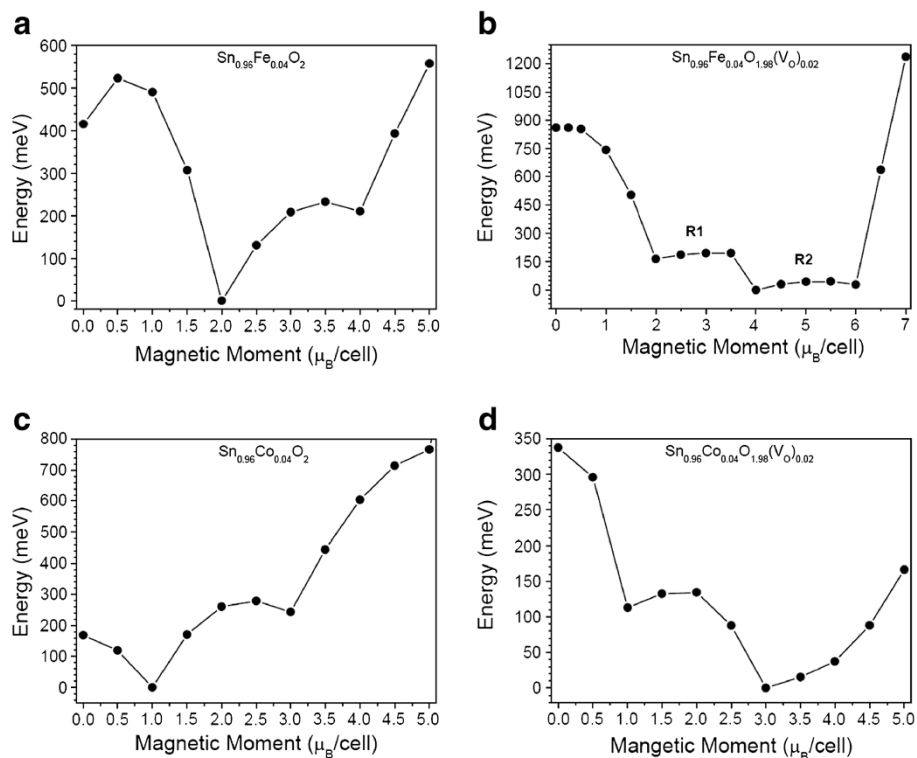


**Figure 1** Total energy vs. magnetic moment per cell. For (a)  $\text{Sn}_{0.96}\text{Fe}_{0.04}\text{O}_2$ , (b)  $\text{Sn}_{0.96}\text{Fe}_{0.04}\text{O}_{1.98}(\text{V}_o)_{0.02}$ , (c)  $\text{Sn}_{0.96}\text{Co}_{0.04}\text{O}_2$ , and (d)  $\text{Sn}_{0.96}\text{Co}_{0.04}\text{O}_{1.98}(\text{V}_o)_{0.02}$ . The total energy of the high-spin ground state is set to zero.

and a magnetic metastable at  $m = 1 \mu_B/\text{cell}$  is seen, with a crossover barrier energy of  $E_S^{1/3} = 21 \text{ meV}$  from  $m = 1$  to  $3 \mu_B/\text{cell}$ .

A better understanding of the behavior for the magnetic moment can be obtained if we analyze the oxidation states of the TM and of the neighbor atoms around it. For the  $\text{Sn}_{0.96}\text{Fe}_{0.04}\text{O}_2$  alloy, the  $\text{Fe}^{4+}$  ( $3d^4$ ) impurity replacing  $\text{Sn}^{4+}$  allows the magnetic states  $m = 0, 2$ , and  $4 \mu_B/\text{cell}$ . In this case, the neighborhood does not contribute to the magnetization of the system. When an oxygen vacancy is taken into account, the impurity state changes from  $\text{Fe}^{4+}$  to  $\text{Fe}^{3+}$  ( $3d^5$ ) and to  $\text{Fe}^{2+}$  ( $3d^6$ ), and the neighboring atoms contribute to the magnetization of the system. For  $m = 2 \mu_B/\text{cell}$ , the oxidation state is  $\text{Fe}^{3+}$  where four spin-up and one spin-down electrons from Fe plus one spin-down electron arising from the neighboring atoms allow for the metastable state (with  $m = 2 \mu_B/\text{cell}$ ). For the  $m = 4$  and  $6 \mu_B/\text{cell}$ , the oxidation state is  $\text{Fe}^{2+}$  where five spin-up and one spin-down electrons from Fe originate the state  $m = 4 \mu_B/\text{cell}$ , while five spin-up and one spin-down electrons from Fe plus two spin-up electrons arising from the neighboring atoms allow the metastable state with  $m = 6 \mu_B/\text{cell}$ . These findings are in agreement with the experimental data [27-30].

Likewise, for the  $\text{Sn}_{0.96}\text{Co}_{0.04}\text{O}_2$  dilute magnetic alloy, the  $\text{Co}^{4+}$  ( $3d^5$ ) and  $\text{Co}^{3+}$  ( $3d^6$ ) impurity replacing  $\text{Sn}^{4+}$  give rise to the magnetic states  $m = 1$  and  $3 \mu_B/\text{cell}$ , respectively. For  $m = 1 \mu_B/\text{cell}$ , three spin-up and two spin-down electrons from cobalt and for  $m = 3 \mu_B/\text{cell}$  four spin-up and two spin-down electrons from cobalt plus one spin-up electron arising from the neighboring atoms allow this metastable state. The states  $\text{Co}^{3+}$  ( $3d^6$ ) and  $\text{Co}^{2+}$  ( $3d^7$ ) are possible when an oxygen vacancy is taken into account for  $m = 1$  and  $3 \mu_B/\text{cell}$ , respectively. For  $m = 1 \mu_B/\text{cell}$ , four spin-up and two spin-down electrons plus one spin-down electron from neighboring atoms are involved. For  $m = 3 \mu_B/\text{cell}$ , five spin-up and two spin-down electrons from cobalt give rise to this metastable state. Experimental studies have confirmed the incorporation of  $\text{Co}^{2+}$  cations into the rutile  $\text{SnO}_2$  lattice [31].

As observed previously for the chromium impurity [26], for iron and cobalt we also observe a relationship between the structural modification around the TM atom, due to the electronic and ionic relaxations, and the occurrence of the magnetic metastability. If we consider a spherical volume involving the TM whose radius is an average distance between the TM and the six oxygen nearest neighbors, our calculations showed that,

after full relaxation, the corresponding volume is reduced. For Co, the volume is reduced by about 16% for the HS state ( $2 \mu_B/\text{cell}$ ) and by 17.5% for the LS state ( $0 \mu_B/\text{cell}$ ). Considering the oxygen vacancy, for the HS states ( $2$  and  $4 \mu_B/\text{cell}$ ) the volume reductions, after full relaxed calculations, were 20% and 22%, respectively, while for the LS state ( $0 \mu_B/\text{cell}$ ), it was 31%. For LS configurations, the presence of an oxygen vacancy allows greater relaxations which reduce the total energy of the system lowering the energy barrier for the crossover. As shown in Figure 2a for Fe, the volume is reduced by about 19% for the states  $m = 0$  and  $2 \mu_B/\text{cell}$ , and by 14% for the state  $m = 4 \mu_B/\text{cell}$ . If the oxygen vacancy is present, the volume around the Fe impurity is reduced by about 19% for the magnetic moment between  $2$  and  $3.5 \mu_B/\text{cell}$ , region R1, and by 12% for the range between  $4$  and  $6 \mu_B/\text{cell}$ , region R2, shown in Figure 2b, both corresponding to an almost flat region. For the cobalt

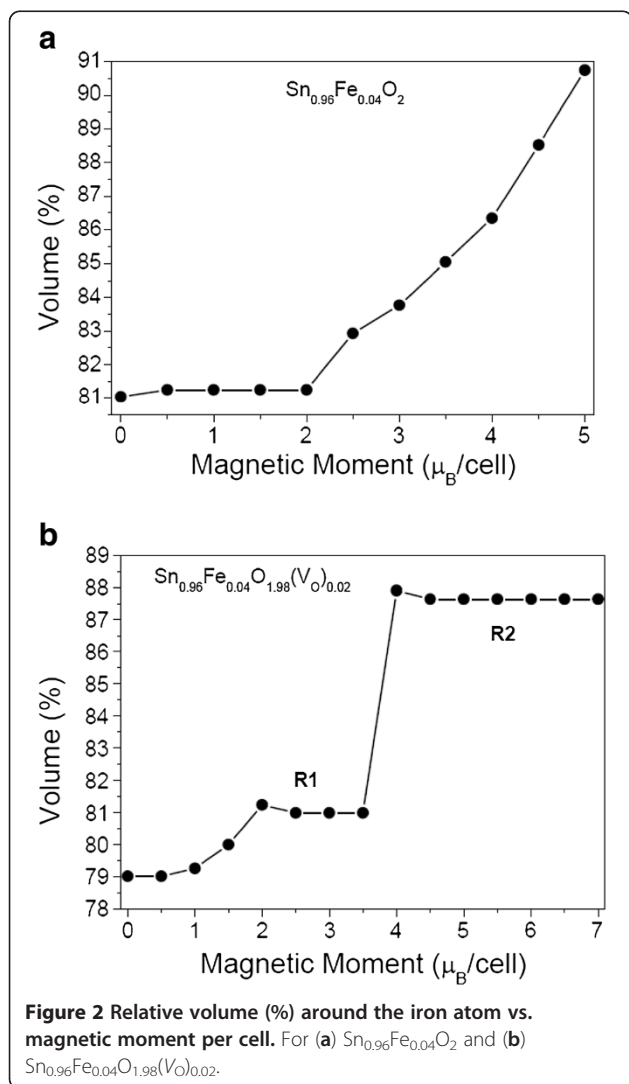
impurity, the volume around Co is reduced by about 19% for the state  $m = 1 \mu_B/\text{cell}$  and by 15% for the state  $m = 3 \mu_B/\text{cell}$ . Considering an oxygen vacancy near the Co atom, the volume is reduced by about 19% for the state  $m = 1 \mu_B/\text{cell}$  and by 11% for the state  $m = 3 \mu_B/\text{cell}$ . The observed magnetic metastability in the DMOs studied here is attributed to a structural modification (relaxations) around the TM impurity. The presence or absence of magnetism in this case is determined by a competition between intra-atomic exchange interactions and inter-atomic electronic motion due to the crystalline field [32]. Therefore, the occurrence of the LS and HS states depends on the effective balance between these two interaction fields. The LS state occurs when the crystal field splitting is larger than the intra-atomic exchange splitting (lowest volume); otherwise, the HS state is the ground state (highest volume).

The ground state total and projected density of states of the Fe  $3d$  orbital are shown in Figure 3a,b for  $\text{Sn}_{0.96}\text{Fe}_{0.04}\text{O}_2$  and  $\text{Sn}_{0.96}\text{Fe}_{0.04}\text{O}_{1.98}(\text{V}_\text{O})_{0.02}$  alloys, respectively. The vertical lines represent the energy values of the highest occupied states for the majority and minority spins. For both cases, the iron  $3d$ -derived states are found to lie in the gap region, showing a half-metallic behavior. For  $\text{Sn}_{0.96}\text{Co}_{0.04}\text{O}_2$  and  $\text{Sn}_{0.96}\text{Co}_{0.04}\text{O}_{1.98}(\text{V}_\text{O})_{0.02}$  alloys, the DOS are shown in Figure 3c,d, respectively. For all cases, we observe a strong character arising from the  $3d$  orbital near the gap region. This feature is also responsible for the half-metallic behavior displayed by the DMOs studied here.

## Conclusions

The influence of the oxygen vacancy in the magnetic and electronic properties of iron and cobalt as impurities in a DMO configuration in rutile  $\text{SnO}_2$  was studied using first principle calculations performed within the spin-density functional theory. A magnetic metastability was observed for both impurity cases. Energy barriers were obtained for the spin crossover between the  $m = 0$  and  $2 \mu_B/\text{cell}$  and between the  $m = 2$  and  $4 \mu_B/\text{cell}$  states in  $\text{Sn}_{0.96}\text{Fe}_{0.04}\text{O}_2$ . For  $\text{Sn}_{0.96}\text{Co}_{0.04}\text{O}_2$ , the observed magnetic metastability and energy barrier were obtained for the spin crossover between the  $m = 3$  and  $1 \mu_B/\text{cell}$  states.

When an oxygen vacancy is considered as one of the six first neighbors to the Fe and Co impurities in these alloys ( $\text{Sn}_{0.96}\text{Fe}_{0.04}\text{O}_{1.98}(\text{V}_\text{O})_{0.02}$  and  $\text{Sn}_{0.96}\text{Co}_{0.04}\text{O}_{1.98}(\text{V}_\text{O})_{0.02}$ ), a considerable modification is observed in the magnetic metastability behavior, with new allowed states appearing for iron. For the cobalt impurity, the presence of an oxygen vacancy promoted a ground state exchange between the magnetic state  $1$  and  $3 \mu_B/\text{cell}$ . This behavior is attributed to the relative contributions of the intra-atomic exchange interaction effects and the



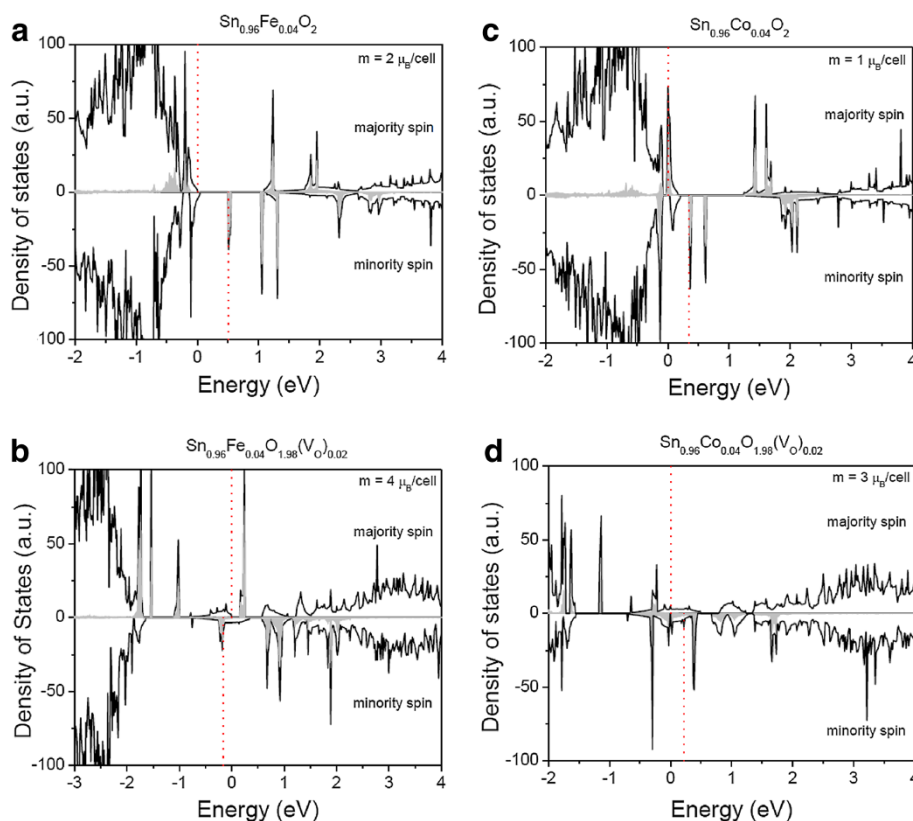


**Figure 3** The ground state total (black lines) and projected (gray shaded areas) density of states. The transition metal 3d-derived states for the majority and minority spins for the ground state magnetic moment are shown for (a)  $\text{Sn}_{0.96}\text{Fe}_{0.04}\text{O}_2$ , (b)  $\text{Sn}_{0.96}\text{Fe}_{0.04}\text{O}_{1.98}(\text{V}_{0.02})$ , (c)  $\text{Sn}_{0.96}\text{Co}_{0.04}\text{O}_2$ , and (d)  $\text{Sn}_{0.96}\text{Co}_{0.04}\text{O}_{1.98}(\text{V}_{0.02})$ . The vertical dashed lines correspond to the highest occupied energy level for the majority and minority spins.

inter-atomic electron motion effects due to the crystal-line field, which are responsible for the relaxations around the TM impurities. Finally, to manipulate the electron spin opens new possibilities to engineering new spintronic devices, and TM-doped DMOs are potential candidates to represent a new kind of material, which display magnetic metastability, SCO phenomena, and a half-metallic behavior.

#### Competing interests

The authors declare that they have no competing interests.

#### Authors' contributions

PDB performed the *ab initio* calculations, participated in the analysis, and drafted the manuscript. LMRS and PDB conceived of the study. HWLA, EFS, LVCA, and LMRS participated in the analysis and in the production of the final version of the manuscript. All authors read and approved the final manuscript.

#### Authors' information

PDB is an assistant professor at the Universidade Federal de Viçosa. LMRS is a senior lecturer and research professor at Texas State University-San Marcos. HWLA is an associate professor at Universidade Federal de São João del Rei. EFS is an associate professor at Universidade Federal de Pernambuco. LVCA is an associate professor at Universidade de São Paulo.

#### Acknowledgments

The authors thank the support received from the Brazilian research financial agencies CNPq (grant nos. 564.739/2010-3/NanoSemiCon, 302.550/2011-9/PQ, 470.998/2010-5/Univ, 472.312/2009-0/PQ, 303578/2007-6/PQ, and 577.219/2008-1/JP), CAPES, FACEPE (grant no. 0553 to 1.05/10/APQ), FAPEMIG, and FAPESP. LS also acknowledge the partial support from the Materials Science, Engineering and Commercialization Program of Texas State University.

#### Author details

<sup>1</sup>Instituto de Ciências Exatas e Tecnológicas, Universidade Federal de Viçosa - CRP, Rio Paranaíba, Minas Gerais CP 38810-000, Brazil. <sup>2</sup>Department of Physics, Texas State University, San Marcos, TX 78666, USA. <sup>3</sup>Departamento de Ciências Naturais, Universidade Federal de São João Del Rei, CP 110, São João Del Rei, Minas Gerais 36301-160, Brazil. <sup>4</sup>Departamento de Física, Universidade Federal de Pernambuco, Recife, Pernambuco 50670-901, Brazil. <sup>5</sup>Instituto de Física, Universidade de São Paulo, São Paulo 05315-970, Brazil.

Received: 9 July 2012 Accepted: 15 September 2012

Published: 28 September 2012

#### References

- Mathew X, Enriquez JP, Mejía-García C, Contreras-Puente G, Cortes-Jacome MA, Toledo Antonio JA, Hays J, Punnoose A: **Structural modifications of  $\text{SnO}_2$  due to the incorporation of Fe into the lattice.** *J Appl Phys* 2006, **100**:073907-1–073907-7.
- Kimura H, Fukumura T, Kawasaki M, Inaba K, Hasegawa T, Koinuma H: **Rutile-type oxide-diluted magnetic semiconductor: Mn-doped  $\text{SnO}_2$ .** *Appl Phys Lett* 2002, **80**:94–96.



3. Wang W, Wang Z, Hong Y, Tang J, Yu M: **Structure and magnetic properties of Cr/Fe-doped SnO<sub>2</sub> thin films.** *J Appl Phys* 2006, **99**:08M115-1–08M115-3.
4. Ogale SB, Choudhary RJ, Buban JP, Lofland SE, Shinde SR, Kale SN, Kulkarni VN, Higgins J, Lanci C, Simpson JR, Browning ND, Das Sarma S, Drew HD, Greene RL, Venkatesan T: **High temperature ferromagnetism with a giant magnetic moment in transparent Co-doped SnO<sub>2-x</sub>.** *Phys Rev Lett* 2003, **91**:077205-1–077205-1.
5. Torres CER, Errico L, Golmar F, Navarro AMM, Cabrera AF, Duhalde S, Sánchez FH, Weissmann M: **The role of the dopant in the magnetism of Fe-doped SnO<sub>2</sub> films.** *J Magn Magn Mater* 2007, **316**:e219–e222.
6. Batzill M, Burst JM, Diebold U: **Pure and cobalt-doped SnO<sub>2</sub>(101) films grown by molecular beam epitaxy on Al<sub>2</sub>O<sub>3</sub>.** *Thin Solid Films* 2005, **484**:132–139.
7. Van Komen C, Thurber A, Reddy KM, Hays J, Punnoose A: **Structure–magnetic property relationship in transition metal (M = V, Cr, Mn, Fe, Co, Ni) doped SnO<sub>2</sub> nanoparticles.** *J Appl Phys* 2008, **103**:07D141-1–07D141-3.
8. Hong NH, Sakai J, Prellier W, Hassini A: **Transparent Cr-doped SnO<sub>2</sub> thin films: ferromagnetism beyond room temperature with a giant magnetic moment.** *J Phys Condens Matter* 2005, **17**:1697.
9. Fitzgerald CB, Venkatesan M, Dorneles LS, Gunning R, Stamenov P, Coey JMD, Stampe PA, Kennedy RJ, Moreira EC, Sias US: **Magnetism in dilute magnetic oxide thin films based on SnO<sub>2</sub>.** *Phys Rev B* 2006, **74**:115307-1–115307-10.
10. Chen W, Li J: **Magnetic and electronic structure properties of Co-doped SnO<sub>2</sub> nanoparticles synthesized by the sol–gel-hydrothermal technique.** *J Appl Phys* 2011, **109**:083930-1–083930-4.
11. Sharma A, Varshney M, Kumar S, Verma KD, Kumar R: **Magnetic properties of Fe and Ni doped SnO<sub>2</sub> nanoparticles.** *Nanomater Nanotechnol* 2011, **1**:29–33.
12. Sharma A, Singh AP, Thakur P, Brookes NB, Kumar S, Lee CG, Choudhary RJ, Verma KD, Kumar R: **Structural, electronic, and magnetic properties of Co doped SnO<sub>2</sub> nanoparticles.** *J Appl Phys* 2010, **107**:093918.
13. Singhal RK, Samariya A, Xing YT, Kumar S, Dolia SN, Deshpande UP, Shripathi T, Saitovitch EB: **Electronic and magnetic properties of Co-doped ZnO diluted magnetic semiconductor.** *J Alloys and Compounds* 2010, **496**:324–330.
14. Singhal RK, Samariya A, Kumar S, Xing YT, Jain DC, Deshpande UP, Shripathi T, Saitovitch E, Chen CT: **On the longevity of H-mediated ferromagnetism in Co doped TiO<sub>2</sub>: a study of electronic and magnetic interplay.** *Solid State Commun* 2010, **150**:1154–1157.
15. Singhal RK, Samariya A, Kumar S, Xing YT, Jain DC, Dolia SN, Deshpande UP, Shripathi T, Saitovitch EB: **Study of defect-induced ferromagnetism in hydrogenated anatase TiO<sub>2</sub>:Co.** *J Appl Phys* 2010, **107**:113916.
16. Samariya A, Singhal SK, Kumar S, Xing YT, Sharma SC, Kumari P, Jain DC, Dolia SN, Deshpande UP, Shripathi T, Saitovitch E: **Effect of hydrogenation vs. re-heating on intrinsic magnetization of Co doped In<sub>2</sub>O<sub>3</sub>.** *Appl Surf Sci* 2010, **257**:585–590.
17. Singhal RK, Samariya A, Kumar S, Sharma SC, Xing YT, Deshpande UP, Shripathi T, Saitovitch E: **A close correlation between induced ferromagnetism and oxygen deficiency in Fe doped In<sub>2</sub>O<sub>3</sub>.** *Appl Surf Sci* 2010, **257**:1053–1057.
18. Hays J, Punnoose A, Baldner R, Engelhard MH, Peloquin J, Reddy KM: **Relationship between the structural and magnetic properties of Co-doped SnO<sub>2</sub> nanoparticles.** *Phys Rev B* 2005, **72**:075203-1–075203-7.
19. Misra SK, Andronenko SI, Rao S, Bhat SV, Van Komen C, Punnoose A: **Cr<sup>3+</sup> electron paramagnetic resonance study of Sn<sub>1-x</sub>Cr<sub>x</sub>O<sub>2</sub> (0.00 ≤ x ≤ 0.10).** *J Appl Phys* 2009, **105**:07C514-1–07C514-3.
20. Coey JMD, Venkatesan M, Fitzgerald CB: **Donor impurity band exchange in dilute ferromagnetic oxides.** *Nat Mater* 2005, **4**:173–179.
21. Cui XY, Delley B, Freeman AJ, Stampfl C: **Magnetic metastability in tetrahedrally bonded magnetic III-nitride semiconductors.** *Phys Rev Lett* 2006, **97**:016402-1–016402-4.
22. Kresse G, Furthmuller J: **Efficiency of ab-initio total energy calculations for metals and semiconductors using a plane-wave basis set.** *Comput Mater Sci* 1996, **6**:15.
23. Kresse G, Furthmuller J: **Efficient iterative schemes for ab initio total-energy calculations using a plane-wave basis set.** *Phys Rev B* 1996, **54**:11169.
24. Perdew JP, Burke K, Ernzerhof M: **Generalized gradient approximation made simple.** *Phys Rev Lett* 1996, **77**:3865.
25. Borges PD, Scolfaro LMR, Leite Alves HW, da Silva EF Jr: **DFT study of the electronic, vibrational, and optical properties of SnO<sub>2</sub>.** *Theor Chem Acc* 2010, **126**:39–44.
26. Borges PD, Scolfaro LMR, Leite Alves HW, da Silva EF Jr, Assali LVC: **Magnetic and electronic properties of Sn<sub>1-x</sub>Cr<sub>x</sub>O<sub>2</sub> diluted alloys.** *Mater Sci Eng B* 2011, **176**:1378–1381.
27. Fitzgerald CB, Venkatesan M, Douvalis AP, Huber S, Coey JMD, Bakas T: **SnO<sub>2</sub> doped with Mn, Fe or Co: room temperature dilute magnetic semiconductors.** *J Appl Phys* 2004, **95**:7390–7392.
28. Sánchez LC, Calle AM, Arboleda JD, Osorio J, Nomura K, Barrero CA: **Fe-doped SnO<sub>2</sub> obtained by mechanical alloying.** *Microelectronics J* 2008, **39**:1320.
29. Xue-Yun Z, Shi-Hui G, Xiu-Feng H, Ya-Lu Z, Yu-Hua X, Zhen-Chao W, Li Z, Ming-Jie L: **Role of defects in magnetic properties of Fe-doped SnO<sub>2</sub> films fabricated by the sol–gel method.** *Chin Phys B* 2009, **18**:4025–4029.
30. Beltran JJ, Sánchez LC, Osorio J, Tirado L, Baggio-Saitovitch EM, Barrero CA: **Crystallographic and magnetic properties of Fe-doped SnO<sub>2</sub> nanopowders obtained by a sol–gel method.** *J Mater Sci* 2010, **45**:5002–5011.
31. Liu XF, Sun Y, Yu RH: **Role of oxygen vacancies in tuning magnetic properties of Co-doped SnO<sub>2</sub> insulating films.** *J Appl Phys* 2007, **101**:123907-1–123907-6.
32. Moruzzi VL: **Singular volume dependence of transition-metal magnetism.** *Phys Rev Lett* 1986, **57**:2211–2214.

doi:10.1186/1556-276X-7-540

**Cite this article as:** Borges et al.: Study of the oxygen vacancy influence on magnetic properties of Fe- and Co-doped SnO<sub>2</sub> diluted alloys. *Nanoscale Research Letters* 2012 **7**:540.

**Submit your manuscript to a SpringerOpen® journal and benefit from:**

- Convenient online submission
- Rigorous peer review
- Immediate publication on acceptance
- Open access: articles freely available online
- High visibility within the field
- Retaining the copyright to your article

Submit your next manuscript at ► [springeropen.com](http://springeropen.com)